PNAS RESEARCH ARTICLE | MEDICAL SCIENCES

RHOA controls oncogenic B cell receptor signaling in aggressive lymphoma

Ariana N. Jacobs[a,b,1], Dominique Jahn[b,c,1], Tim Beringer[a,b], Sebastian Wolf[a,b], Ramesh K. Krishnan[b,c], Michael Engelke[d], Björn Häupl[b,c], Silvia Münch[a,b], Niklas Dienstbier[a,b], Martine Pape[a,b], Marion Bodach[b,c], Xin Yu[e], Nazli Serin[f], Rebecca Wurm-Kuczera[f], Alena Zindel[b,c], Carmen Döbele[b,c], Björn Chapuy[f], Louis M. Staudt[e,2], Sebastian Scheich[a,b,c,g,2], and Thomas Oellerich[a,b,c,g,2]

Affiliations are included on p. 8.

Contributed by Louis Staudt; received December 1, 2025; accepted December 30, 2025; reviewed by Michael R. Green and Shiv Pillai

Diffuse large B cell lymphoma (DLBCL) is characterized by a variety of specific genetic alterations that impact signaling pathway dependencies and therapeutic outcomes. Among the recurrently mutated genes, we identified *RHOA*, a member of the small GTPase family, as a selective dependency in DLBCL. Here, we show that RHOA function is essential for the survival of ABC DLBCL cells because it sustains oncogenic B cell receptor (BCR) signaling through maintaining a signaling-permissive conformation of the cortical actin network. This enables the formation of active BCR microclusters at the cell surface, ultimately resulting in constitutive, BCR-driven NF-κB survival signaling. Moreover, we found that RHOA controlled endocytosis of the BCR and thereby the assembly of the endolysosomal My–T–BCR multiprotein complex, a central activator of NF-κB consisting of MYD88, Toll-like receptor 9, and the internalized BCR. The recurrent DLBCL-associated *RHOA* R5W mutation rendered RHOA constitutively active in its GTP-bound state and changed the conformation of the actin network from primarily filamentous actin to globular actin. This altered actin state led to an increase in BCR microcluster formation, amplification of NF-κB signaling, and resistance to inhibitors targeting chronic active BCR signaling. Hence, our study establishes RHOA and its mutant isoforms as critical regulators of oncogenic BCR signaling in DLBCL.

lymphoma | DLBCL | RHOA | cytoskeleton | B cell receptor

Significance

B cell receptor (BCR) signaling is an important survival pathway in diffuse large B cell lymphoma (DLBCL). We show that the small GTPase RHOA controls lymphoma cell survival by rewiring the cortical actin cytoskeleton network, thereby inducing BCR microcluster formation at the cell surface and My-T-BCR complex assembly in the endolysosomal compartment, both being essential for oncogenic NF-κB signaling. Our findings explain the pathogenic role of RHOA gain-of-function mutations and underline their contribution to the pathogenesis of aggressive lymphomas.

Diffuse large B cell lymphoma (DLBCL) is the most common type of non-Hodgkin's lymphoma (1, 2). Gene expression profiling has uncovered two distinct cell-of-origin subtypes, activated B cell–like (ABC) and germinal center B cell–like (GCB) DLBCL, that differ in their molecular signaling mechanisms and therapy response to chemoimmunotherapy (2). The ABC subtype is characterized by self-antigen-driven, chronic active BCR signaling, reflected by microclustering of the BCR on the cell surface (3). Chronic BCR activation triggers multiple intracellular signaling cascades including NF-κB, which is a key survival pathway in ABC DLBCL (4). BCR-dependent activation of NF-κB requires a complex interplay of specific kinases and adapter proteins. These include spleen tyrosine kinase (SYK), Bruton's tyrosine kinase (BTK), and protein kinase C-beta (PKCβ) that promote the assembly of the CARD11-BCL10-MALT1 (CBM) adapter protein complex as an activator of IκB kinase (IKK) (5). IKK-mediated phosphorylation of the inhibitory factor IκBα leads to its proteasomal degradation and the subsequent release of NF-κB subunits that translocate into the nucleus to regulate gene expression (6). More recent studies exploring the genomic landscape of DLBCL have identified multiple genetic subtypes (7–10). The MCD genetic subtype, which is genetically primarily found in ABC DLBCL, is enriched for mutations in the BCR component CD79B and the immune adapter MYD88 ($MYD88^{L265P}$). $MYD88^{L265P}$ associates with Toll-like receptor 9 and the internalized BCR in the endolysosomal compartment within the so-called My-T-BCR complex that serves as an activator of oncogenic NF-κB signaling in MCD tumors (11). In contrast, GCB DLBCL is characterized by a different mutation spectrum and depends on "toncogenic" BCR signaling that is likely ligand-independent and engages primarily the PI3K/AKT pathway (5).

With the advent of the recent genetic characterization of DLBCL, our understanding of disease biology has expanded considerably. However, the genomic landscape is highly complex and heterogeneous (8–10), and the majority of mutations remain poorly characterized at the functional level. Among the recurrently mutated genes, we identified *Ras Homolog Family Member A* (*RHOA*), which harbors distinct hotspot mutations in DLBCL tumors compared to those described in T cell lymphoma. RHOA is a small GTPase that cycles between an active GTP-bound and inactive GDP-bound state to regulate diverse cellular

Competing interest statement: R.W.-K. received honoraria from BMS, Gilead, Hexal, Roche, Kite and Sobi B.C. is an inventor on patent applications related to DLBclass. B.C. is the lead clinical and scientific investigator on the ITT R-Pola-Glo study supported by IKF and Roche. B.C. served unrelated to the submitted work on advisory boards for AbbVie, AstraZeneca, ADC, Bristol Myers Squibb, Gilead, Incyte, J&J, Regeneron, Roche, and Sobi, and received honoraria unrelated to the submitted work for talks from AbbVie, Ars tempi, AstraZeneca, BMS, Gilead, Incyte, Janssen, KML, ONO, Roche, Sandoz, and Sobi. B.C. received travel support from ONO, Roche and Sobi. S.S.: Honoraria: BMS, AstraZeneca, AbbVie, Incyte T.O. served on advisory boards for and/or received honoraria from AbbVie, BeiGene, Bristol Myers Squibb, Gilead, Janssen, Kite, Kronos Bio, Lilly, Roche, and Sobi. T.O. received travel support from BeiGene, Janssen, Kite, and Roche. S.W. received travel support from Jazz Pharmaceuticals, Servier, and AbbVie, and served on advisory boards for AbbVie, Servier, Daiichi Sankyo, Astellas, and Stemline. S.W. was supported by the Mildred-Scheel-Nachwuchszentrum (MSNZ) of the German Cancer Aid and the INITIALISE Advanced Clinician Scientist program of the Federal Ministry of Research, Technology and Space (BMFTR).

[1]A.N.J. and D.J. contributed equally to this work.

[2]To whom correspondence may be addressed. Email: lstaudt@mail.nih.gov, s.scheich@med.uni-frankfurt.de, or oellerich@em.uni-frankfurt.de.

This article contains supporting information online at https://www.pnas.org/lookup/suppl/doi:10.1073/pnas.2534531123/-/DCSupplemental.

Published January 27, 2026.

processes such as cytoskeletal organization, cell migration, signaling, and cell cycle progression (12). The molecular role of *RHOA* and its mutant variants has not been explored in DLBCL. Here, we elucidate the function of RHOA as a key regulator of oncogenic BCR signaling, thereby providing insights into the functional interplay between actin cytoskeleton dynamics, spatial BCR organization, and downstream oncogenic BCR signaling in ABC DLBCL.

Results

RHOA Controls NF-κB-Dependent Survival Signals in ABC DLBCL. Functional genomic screens have emerged as a powerful tool to identify cellular dependencies on specific genes and pathways. Using genome-wide CRISPR-Cas9 screens, we identified *RHOA* as a dependency in lymphoma cells (11, 13–15) (Fig. 1*A*), which was confirmed in the publicly available DepMap database (16) that aggregates data from more than 1,100 CRISPR screens in more than 160 cancer entities (Fig. 1*B*). We identified lymphoma as one of the most RHOA-dependent cancer entities, and among the lymphoid malignancies, DLBCL showed the strongest reliance on RHOA compared to B-ALL, T-NHL, and myeloma cell lines (Fig. 1*B*).

To validate these findings, we evaluated the impact of *RHOA* deletion in a panel of 4 ABC DLBCL, 9 GCB DLBCL, and 4 mantle cell lymphoma (MCL) cell lines. *RHOA* deletion in MCL models showed only a minimal effect on cell survival, while being critical in DLBCL, particularly in ABC DLBCL cell lines (Fig. 1*C*).

To assess the influence of RHOA inhibition on cell survival-promoting signaling pathways, we next utilized the RHOA-specific small molecule inhibitor rhosin (17, 18) and analyzed gene expression changes induced by RHOA inhibition in the DLBCL cell lines HBL1, TMD8, and RIVA. We compared these gene expression profiles with those upon treatment of the same cell lines with the BTK inhibitor ibrutinib. As expected, gene signatures associated with NF-κB activity and proximal BCR signaling were downregulated in ibrutinib-treated cells (Fig. 1*D* and *SI Appendix*, Fig. S1*A* and Datasets S1–S3). Interestingly, RHOA inhibition mimicked these changes reflected by a strong correlation of the transcriptional changes induced by either ibrutinib or rhosin treatment (*SI Appendix*, Fig. S1*B* and Datasets S1–S3).

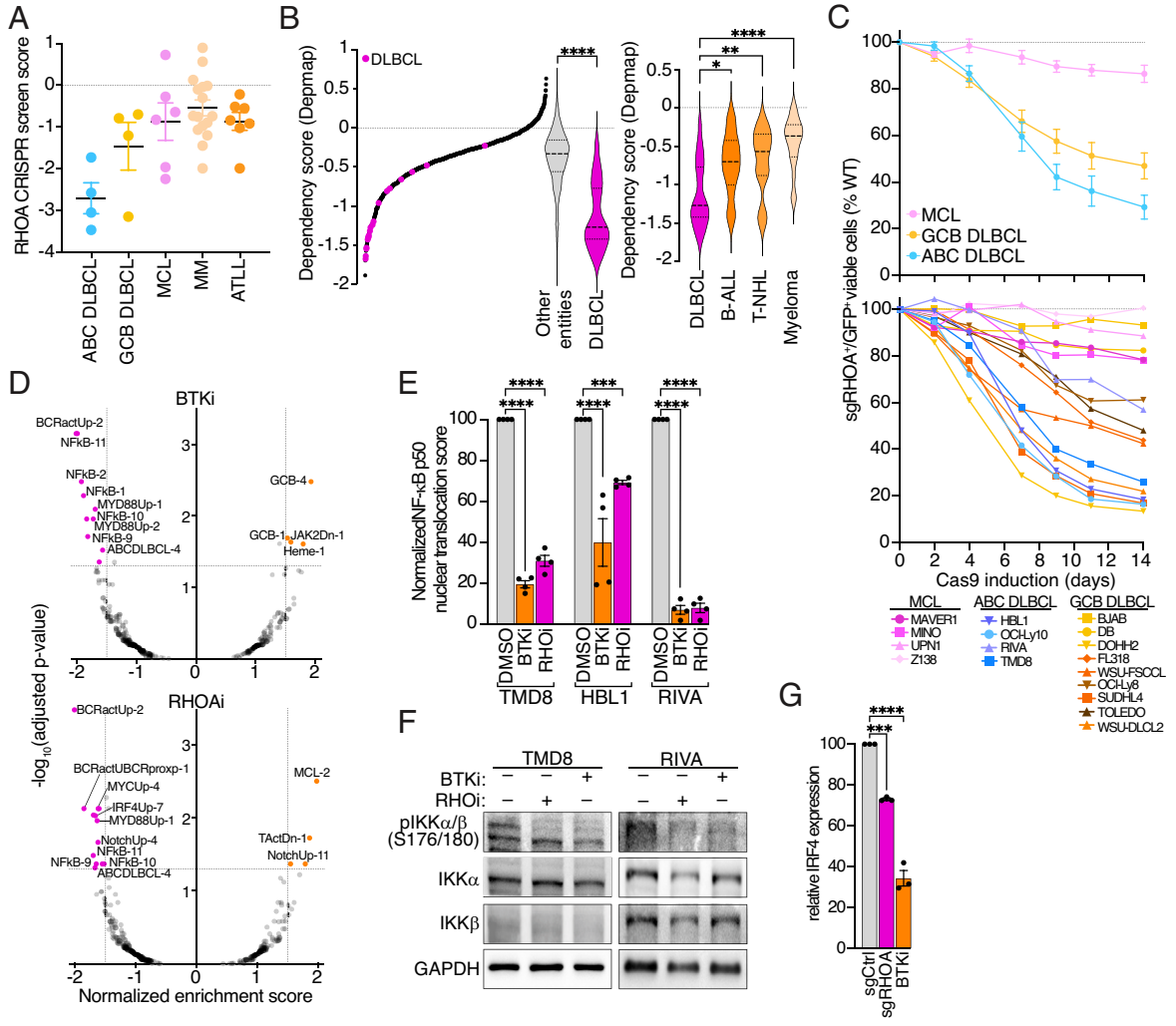

Fig. 1. RHOA is essential in ABC DLBCL and controls NF-κB-mediated survival signaling. (*A*) RHOA CRISPR screen scores (CSS) in different lymphoid malignancies. Mean ± SEM shown. (*B*) *Left*, DepMap essentiality scores of RHOA in DLBCL cell lines compared to other cell line lineages. Box and whiskers: 10 to 90% percentile. ****$P < 0.0001$ (unpaired *t*-test). *Right*, DepMap essentiality scores of RHOA in DLBCL compared to other lymphoid malignancies. Box and whiskers: 10 to 90% percentile. ****$P < 0.0001$, **$P < 0.01$, *$P < 0.05$ (one-way ANOVA). (*C*) *Upper* panel, average toxicity of *RHOA* deletion in ABC DLBCL, GCB DLBCL, and mantle cell lymphoma (MCL) cell lines. *Lower* panel, toxicity of *RHOA* knockout in individual cell lines. Viable cell numbers are normalized to day 0. Mean of at least three replicates per cell line. (*D*) Gene set enrichment analysis using the lymphoma signature database in HBL1 ABC DLBCL cells after treatment with the BTK inhibitor (BTKi) ibrutinib or RHOA inhibitor (RHOi) rhosin for 10 h. (*E*) Imagestream nuclear NF-κB p50 translocation scores in TMD8, HBL1, or RIVA cells after 24 h treatment with RHOi or BTKi. ****$P < 0.0001$, ***$P < 0.001$ (one-way ANOVA). (*F*) Immunoblots of (*Left*) TMD8 and (*Right*) RIVA cells of the indicated proteins after 6 h of treatment with RHOi or BTKi. (*G*) Normalized IRF4-GFP expression measured by flow cytometry after deletion of *RHOA* or BTKi treatment for 16 h.

To confirm the observed NF-κB-specific effects, we tested whether NF-κB activity was altered upon pharmacologic inhibition of RHOA in ABC cell lines. As measured by imaging flow cytometry and immunoblots, NF-κB p50 translocation into the nucleus and phosphorylation of IKK were significantly reduced upon RHOA inhibition (Fig. 1 *E* and *F*). Furthermore, we used engineered TMD8 cells in which GFP was knocked into the endogenous *IRF4* locus. The resulting IRF4–GFP fusion protein served as a robust and direct marker of NF-κB activity (3) and was validated using the BTK inhibitor acalabrutinib that is known to suppress NF-κB in these cells. The genetic deletion of *RHOA* by CRISPR-Cas9 also reduced IRF4–GFP expression indicating dampened NF-κB activity (Fig. 1*G*), further supporting RHOA's role in regulating NF-κB activity and thereby controlling cell survival in ABC DLBCL.

Chronic Active BCR Signaling Depends on RHOA Function. To further elucidate how RHOA controls NF-κB activity, we analyzed tyrosine phosphorylation changes in three ABC cell lines using quantitative phosphoproteomics after either inducible genetic knock-down of *RHOA* or *CD79A*, the latter known to completely disrupt BCR signaling (4). Overall, between 409 and 1,359 phospho-tyrosine sites were quantified in the three ABC cell lines. Silencing of *RHOA*, likewise *CD79A*, decreased phosphorylation of several BCR-proximal signaling effectors including SYK, BTK, PLCγ2, and the adaptor protein BLNK (Fig. 2 *A* and *B* and *SI Appendix*, Fig. S2, and Datasets S4–S6), which we confirmed by immunoblotting (Fig. 2*C*). Overall, the signaling changes were highly correlated between both conditions, indicating that RHOA function is essential for maintaining chronic active BCR signaling in ABC DLBCL. Furthermore, the data suggest that RHOA acts proximal to the BCR, because *RHOA* silencing led to the reduced phosphorylation of SYK and the adaptor protein BLNK that both directly bind to activated BCRs (19, 20).

RHOA Regulates BCR Internalization and Subsequent Formation of the My-T-BCR Complex. Having identified RHOA as a regulator of chronic active BCR signaling, we next explored the underlying mechanisms. First, we identified the proteins that are in proximity to RHOA to gain insight into RHOA's functional interaction with other proteins and pathways. For this purpose, we expressed RHOA–BioID2 fusion proteins in two ABC cell lines allowing the promiscuous biotin ligase BioID2 to biotinylate proteins in close proximity to RHOA, which were read out by mass spectrometry after streptavidin-based affinity purification. We plotted the enrichment score of the individual proteins against their degree of essentiality for cell survival as measured by genome-wide CRISPR-Cas9 screens in the same cell lines, thereby defining its "essential interactome" (11). As expected, RHOA itself and its two associated protein kinases ROCK1 and ROCK2, which mediate RHOA signaling to the actin cytoskeleton (21), were biotinylated. In addition, multiple cell surface receptors which are not essential for ABC DLBCL cell survival (CD86, CD72, CD44, CD20, CD22, and CD19) were biotinylated, likely reflecting RHOA's localization at the inner plasma membrane (22) (Fig. 3*A* and *SI Appendix*, Fig. S3*A* and Datasets S7 and S8). Surprisingly,

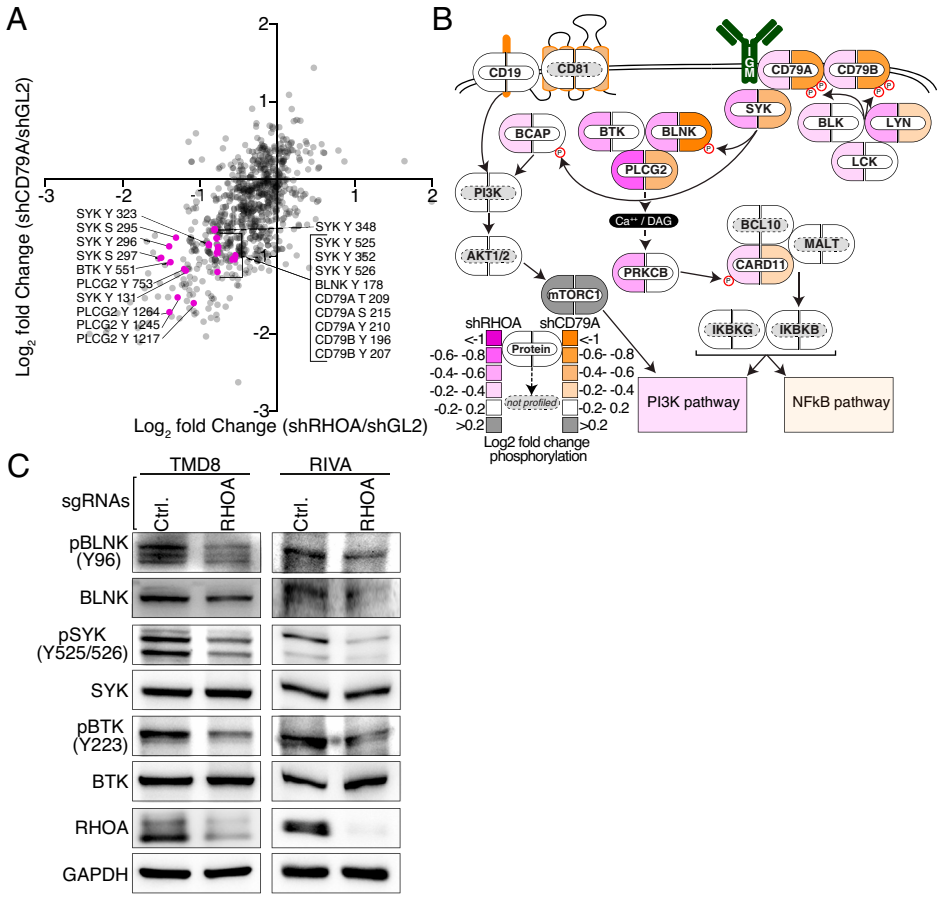

Fig. 2. RHOA controls proximal BCR signaling. (*A*) Changes in global phosphotyrosine abundance in RIVA cells after genetic silencing of *RHOA* (x-axis) or *CD79A* (y-axis). Phosphosites quantified in at least two of three replicates, with a localization probability ≥0.75. (*B*) Diagram of BCR signaling displaying changes in average phosphorylation abundance per protein in three ABC DLBCL cell lines after genetic silencing of *RHOA* (*Left* pill, berry) or *CD79A* (*Right* pill, orange). (*C*) Immunoblots of indicated proteins in TMD8 cells (*Left*) and RIVA cells (*Right*) upon genetic deletion of *RHOA*.

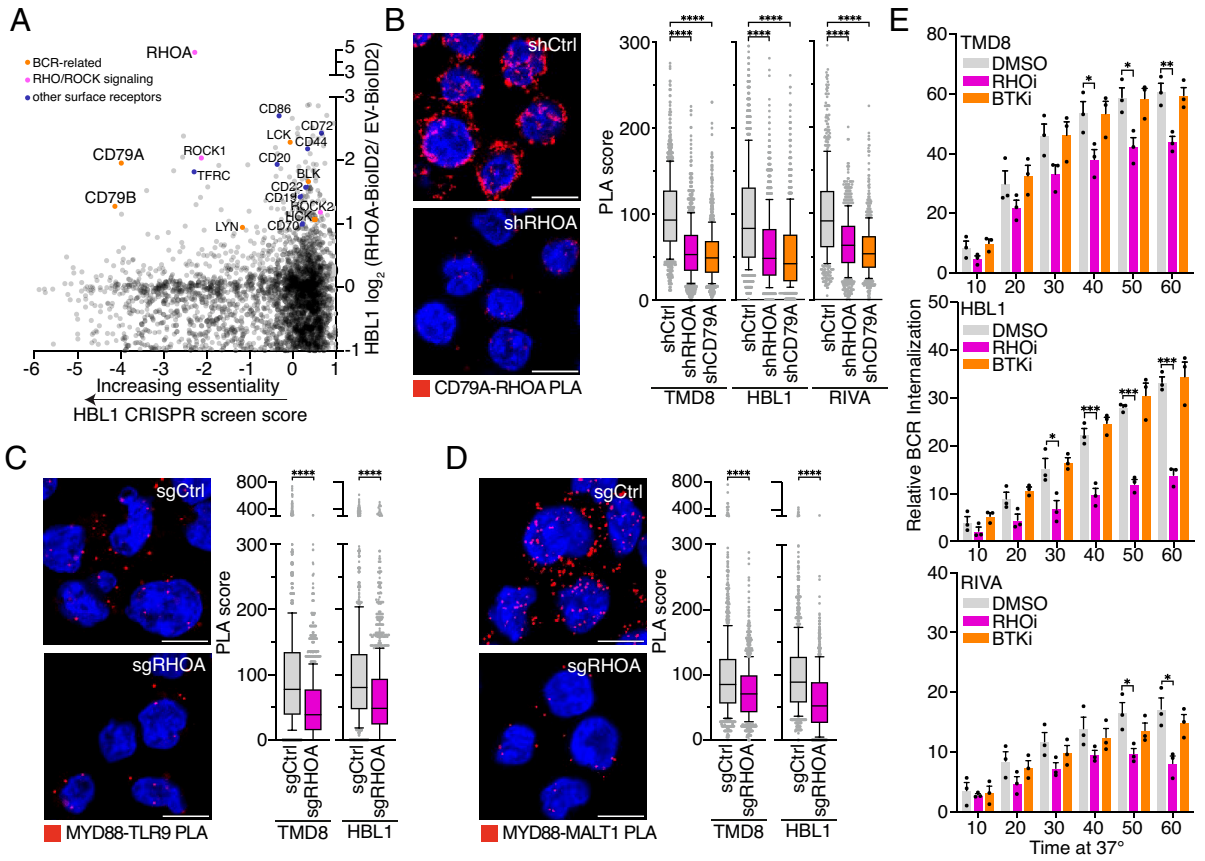

Fig. 3. RHOA drives My-T-BCR formation. (*A*) RHOA interactome in HBL1 cells compared to the CRISPR screen score (CSS). (*B*) *Left*, representative PLA images of RHOA-CD79A pair in TMD8 cells under control or *RHOA* genetic silencing. PLA puncta are shown in red and DAPI in blue. (Scale bar, 10 μm.) *Right*, PLA scores for the RHOA–CD79A PLA pair in TMD8, HBL1, and RIVA cells upon control, *RHOA*, or *CD79A* genetic silencing. Box and whiskers: 10 to 90% percentile. ****P < 0.0001 (one-way ANOVA). (*C* and *D*) *Left*, representative PLA images (n = 3) of (*C*) MYD88 with TLR9 and (*D*) MYD88 with MALT1 in TMD8 and HBL1 cells upon control or *RHOA* genetic deletion. PLA puncta are depicted in red, DAPI in blue. (Scale bar, 10 μm.) *Right*, PLA scores of the respective PLA pairs in TMD8 and HBL1 cells upon nontargeting control or *RHOA* genetic deletion. Box and whiskers plot indicating 10th to 90th percentile. ****P < 0.0001 (one-way ANOVA). (*E*) BCR internalization assay of TMD8, HBL1, and RIVA cells after treatment with a RHOA inhibitor (RHOi) or BTK inhibitor (BTKi) as indicated. ***P < 0.001, **P < 0.01, *P < 0.05 (Mann-Whitney U test).

we identified the BCR subunits CD79A and CD79B as essential regulators of cell survival in proximity to RHOA suggesting that RHOA functionally interacts with the BCR. This notion is further supported by the finding that the degree of the dependency on the BCR subunits CD79A/B, as assessed previously (3), and RHOA significantly correlated across lymphoma cell lines (P = 0.007, r^2 = 0.44; *SI Appendix*, Fig. S3*B*). Notably, and in line with these results, genetic deletion of *RHOA* did not effect the viability of the ABC line OCI-Ly3, in which a gain-of-function CARD11 mutant isoform strongly activates NF-κB, rendering these cells independent of upstream BCR signaling (4, 23) (*SI Appendix*, Fig. S3*C*).

To further validate the interaction of RHOA and the BCR, we visualized the RHOA–CD79A interaction by proximity ligation assays (PLA), a method to detect endogenous protein–protein interactions (24). Across three ABC cell lines, we observed a robust and specific PLA signal validating the interaction of RHOA and the BCR (Fig. 3*B*). Due to evident intracellular PLA signals, we investigated whether RHOA impacts not only the plasma membrane fraction of the BCR, but also the My-T-BCR multiprotein complex that resides in the endolysosomal compartment as a central regulator of cell survival in ABC DLBCL (11). Therefore, we assessed the My-T-BCR complex using MYD88-TLR9 and MYD88-MALT1 PLAs as previously published (11). In both assays, genetic deletion of *RHOA* significantly reduced My-T-BCR formation (P < 0.0001) (Fig. 3 *C* and *D*). Because My-T-BCR formation requires BCR internalization and because this process is dependent on the cytoskeleton (25, 26), we hypothesized that reduced My-T-BCR assembly upon *RHOA* genetic deletion was due to alterations in trafficking of the BCR from the plasma membrane to the endolysosomal compartment. Using a flow cytometry-based BCR internalization assay, we indeed observed a significant reduction of the BCR internalization rate after RHOA inhibition, while treatment with the BTK inhibitor ibrutinib did not affect internalization (Fig. 3*E*).

Taken together, these data suggest that RHOA controls two spatially distinct, yet mechanistically related mechanisms of oncogenic BCR signaling: Surface-level activation, and by subsequent regulation of BCR internalization, the assembly of the My-T-BCR complex in the endolysosomal compartment.

Mutant RHOA Enhances Oncogenic BCR Signaling Through Reorganization of BCR Microclusters. *RHOA* is recurrently mutated in different lymphoid malignancies (7, 8, 27). Interestingly, the single point mutation p.G17V, which occurs in more than 60% of T cell lymphoma patients (27, 28), does not occur in DLBCL tumors (Fig. 4*A*). Instead, in a large survey of DLBCL patients, we identified 312 cases with *RHOA* mutations exhibiting mutational hotspots leading predominantly to arginine 5 (R5), tyrosine 34 (Y34), tyrosine 42 (Y42), and leucine 69 (L69) exchanges (Fig. 4*A*) (7, 8, 15, 29–72). Structural modeling with superimposition of wild-type (WT) and mutant structures revealed that both missense mutations are positioned at the

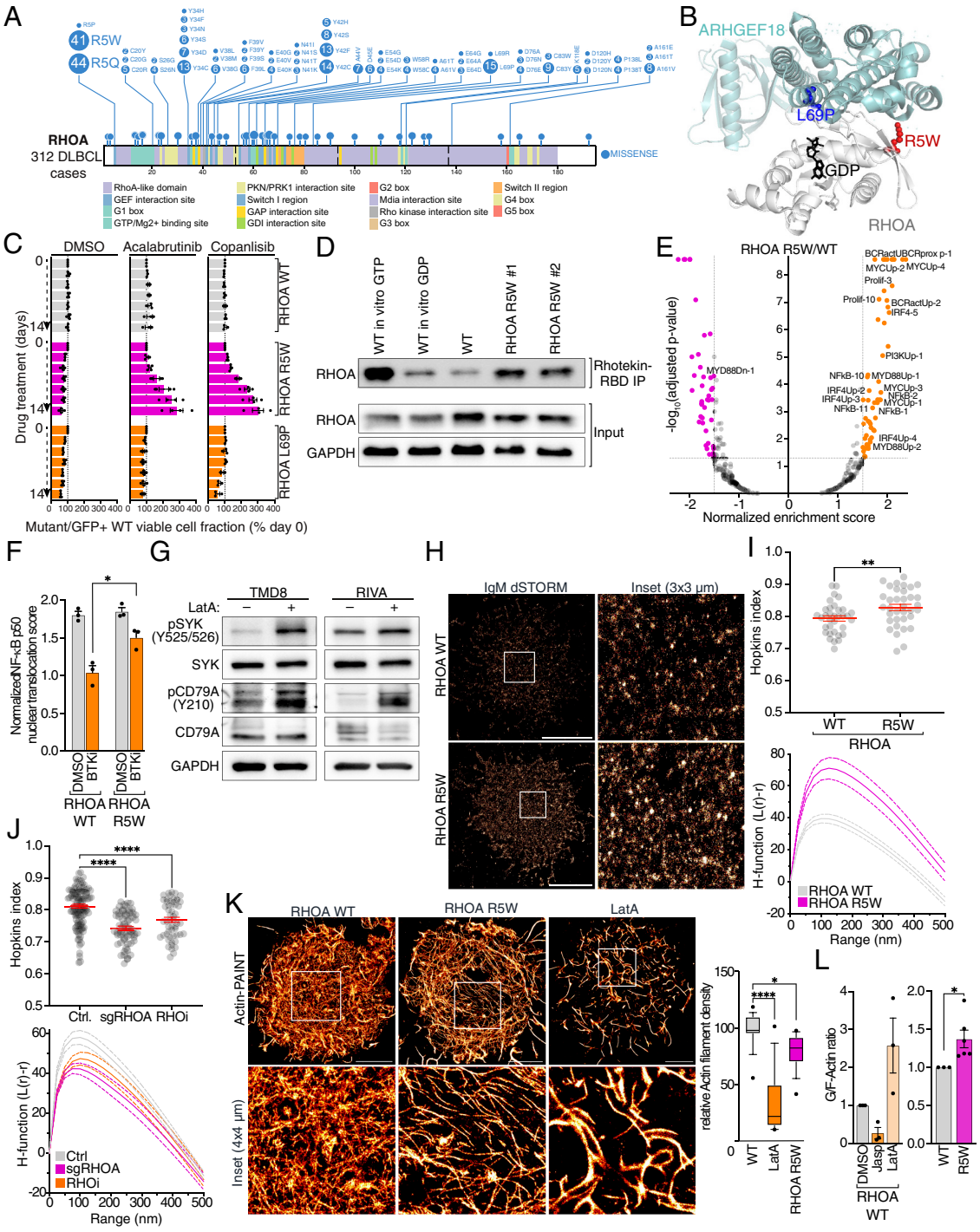

Fig. 4. RHOA mutations alter activity, resistance, and clustering. (*A*) Lollipop plot of RHOA mutation frequencies in DLBCL. (*B*) Costructural model of RHOA (gray, PDB ID: 1DPF) and ARHGEF18 (cyan, PDB:4D0N). Amino acid changes of the indicated missense mutations are overlaid to the RHOA–ARHGEF18 interface and color-coded: L69P, blue; R5W, red. GDP highlights the catalytic center in black. (*C*) Competitive growth experiment where the indicated TMD8 cell genotypes were mixed with GFP+ wild-type (WT) cells under DMSO, acalabrutinib, or copanlisib treatment. GFP was evaluated over the course of 2 wk. Bars display relative GFP negative cells normalized to day 0. Mean of at least 3 independent experiments with SEM depicted as error bars. (*D*) Immunoblots of active RHOA immunoprecipitations in WT RHOA p.R5W TMD8 knock-in cells for the indicated proteins. Upper panel, rhotekin-RBD immunoprecipitations. Lower panel, input controls. (*E*) Gene set enrichment analysis utilizing the lymphoma signature database of TMD8 p.R5W vs WT cells. (*F*) Mean nuclear NF-κB (p50) translocation score evaluated by ImageStream flow cytometry in WT or p.R5W TMD8 cells under DMSO or acalabrutinib treatment for 16 h. $*P < 0.05$ (two-way ANOVA). (*G*) Immunoblots of indicated proteins in TMD8 cells (*Left*) and RIVA cells (*Right*) under 15 min LatA treatment. (*H*) Reconstructed dSTORM IgM single molecule localizations in TMD8 WT (*Upper* panel) and RHOA p.R5W cells (*Lower* panel). The white square in representative images (three or more experiments) indicates inset used for quantification, shown magnified to the *Right*. (Scale bar, 5 μm.) (*I* and *J*) dSTORM quantification of IgM distribution via the Hopkins index (above) and the H-function (below) in WT and RHOA p.R5W TMD8 cells. SEM depicted by error bars (Hopkins index) and dotted lines (H-function). Data are pooled from 3 (*I*) or 2 (*J*) independent experiments. $**P < 0.01$, $****P < 0.0001$ (one-way ANOVA). (*K*) *Left*, Reconstructed Actin-DNA-PAINT single molecule localizations in TMD8 WT cells treated with DMSO (*Left* panel), TMD8 WT cells for 15 min with latrunculin A (LatA, *Right* panel) and TMD8 RHOA p.R5W cells (*Middle* panel). The white square area in representative images shown magnified *Below*. (Scale bar, 3 μm.) *Right*, quantified relative actin filament density of TMD8 WT cells treated with DMSO, TMD8 WT cells for 15 min with latrunculin A (LatA) and TMD8 RHOA p.R5W cells. Box and whiskers: 10 to 90% percentile. $*P < 0.05$, $****P < 0.0001$ (one-way ANOVA). (*L*) Quantification of replicated immunoblots of G-actin/F-actin differential separation assays in (*Left*) TMD8 WT cells after treatment with DMSO, jasplakinolide (Jasp), and latrunculin A and (*Right*) TMD8 WT cells and two independent RHOA p.R5W clones in TMD8 cells as indicated.

interface of RHOA and its activators, specific GEF proteins like ARHGEF18, thus potentially influencing the interaction between RHOA and these proteins (Fig. 4*B*).

We next investigated the distribution of *RHOA* mutations across DLBCL subtypes in large patient cohorts (7, 8, 15, 30–35, 37, 40–45, 48–52, 54, 56, 60–65, 67, 68, 71, 73, 74). Overall, *RHOA* mutations were found in both ABC and GCB DLBCL, and they were most prevalent in the EZB (C3) genetic subtype. The most frequent R5 mutations (R5W/Q) were most enriched in the MCD subtype though (*SI Appendix*, Fig. S4*A*), supporting a potential role of the R5W or R5Q RHOA variants in the regulation of oncogenic BCR and My-T-BCR signaling in this subtype.

To explore the functional role of DLBCL-specific *RHOA* mutations, we generated endogenous knock-in mutants of RHOA (p.R5W and p.L69P) in TMD8 cells and tested competitive growth phenotypes under selective pressure with either the BTK inhibitor acalabrutinib or the PI3-kinase inhibitor copanlisib. Interestingly, expression of the p.R5W variant led to significant outgrowth under BTKi and PI3Ki treatment, while p.L69P knock-in cells demonstrated no growth advantage (Fig. 4*C*). Moreover, higher levels of active GTP-bound RHOA in p.R5W mutants were detected by pull-down assays using RBD-coupled beads, a well-established assay to estimate the amount of active RHOA (75), further validating the observed gain-of-function phenotype of p.R5W RHOA in ABC DLBCL cells (Fig. 4*D*). Consequently, the p.R5W mutant cells were less sensitive to both kinase inhibitors than the RHOA WT cells (*SI Appendix*, Fig. S4*B*).

We next evaluated gene expression changes in p.R5W cells under selective drug pressure and observed an upregulation of gene expression signatures indicating increased NF-κB activity and proximal BCR signaling according to established signatures derived from the *Signature* database (76) (i.e., BCRactUBCRproxp-1, BCRactUp-2, IRF4-5, IRF4-2,-3, MYD88Up-1, and NF-κB-2,-10,-11; Fig. 4*E* and Dataset S9). These signatures were largely overlapping with the signatures that were found to be downregulated upon pharmacological inhibition of RHOA, again supporting the notion that p.R5W results in a gain-of-function. In accordance with the gene expression data, imaging flow cytometry analysis of p.R5W mutant cells showed significantly increased nuclear translocation of NF-κB p50 after acalabrutinib treatment compared to cells expressing WT RHOA (Fig. 4*F*). In contrast, there were no differences in FOXO1 nuclear localization (*SI Appendix*, Fig. S4*C*), a transcriptional repressor mainly acting downstream of AKT (77).

We identified RHOA as a regulator of BCR signaling and internalization (Figs. 2 and 3). Previous studies showed that BCR signals emerge from active BCR microclusters at the cell surface that are controlled by a tightly regulated actin cytoskeleton fence underneath the plasma membrane (25, 26). For example, latrunculin A (LatA), a chemical drug interfering with actin polymerization, was shown to be sufficient to induce BCR signaling by disrupting the cortical actin cytoskeleton network (25). To experimentally test whether LatA can enhance BCR signaling in ABC DLBCL cells, we measured the calcium flux upon BCR stimulation in the presence or absence of LatA. In accordance with published literature, LatA enhanced Ca^{2+} signaling and the phosphorylation of CD79A and SYK (Fig. 4*G* and *SI Appendix*, Fig. S4*D*). In contrast, and in line with our observations, RHOA inhibition compromised the BCR-induced Ca^{2+} mobilization (*SI Appendix*, Fig. S4*D*).

As RHOA is a known regulator of the actin cytoskeleton and since we identified a functional and spatial interaction with the BCR, we next investigated by superresolution microscopy whether the p.R5W mutant form of RHOA impacts BCR cell surface organization and microcluster formation. TMD8 WT and p.R5W mutant cells were stained for IgM and imaged using direct stochastic optical reconstruction microscopy (dSTORM) in total internal reflection fluorescence (TIRF) mode. The fitted molecule localizations were analyzed by the Hopkins index (33), a metric to assess the clustering tendency of molecules, and the H-function, a nearest neighbor metric that estimates clustering tendency and cluster size (78, 79). IgM was clustered on the cell surface of WT TMD8 cells as previously described (3) (Fig. 4*H*) and RHOA p.R5W mutants showed an increased clustering tendency, as demonstrated by the Hopkins index and Ripley's H-function (Fig. 4*I*). Conversely, genetic deletion of *RHOA* or pharmacologic RHOA inhibition significantly decreased BCR clustering (Fig. 4*J*).

Based on these data and the literature describing RHOA's role in actin regulation, we further hypothesized that mutant RHOA impacts BCR clustering through deregulation of the actin cytoskeleton. To test this, we turned once again to superresolution microscopy, specifically DNA-PAINT. WT cells in the presence or absence of LatA, as well as mutant RHOA cells, were stained with an actin dye and imaged in TIRF mode. We skeletonized reconstructed images and calculated summary statistics for actin fiber density. As expected, LatA treatment disrupted the actin filament network (Fig. 4*K*), which was described to trigger BCR signaling (25). Strikingly, RHOA p.R5W mutant cells also displayed a decreased actin filament network (Fig. 4*K*) suggesting that the rewiring of the actin cytoskeleton enhances oncogenic BCR signaling. To biochemically validate these results, we performed differential separation experiments of globular (G)-actin and filamentous (F)-actin in cells treated with either LatA or the F-actin stabilizer Jasplakinolide (Jasp). As expected, LatA treatment shifted the G/F actin ratio toward G-actin, while Jasp treatment skewed it toward F-actin, validating our biochemical read-out (Fig. 4*L* and *SI Appendix*, Fig. S4*E*). In line with the microscopy data, RHOA p.R5W cells displayed, similarly to LatA treatment, a significantly higher G/F actin ratio in this assay, thus providing evidence that RHOA controls BCR microcluster formation and signaling through the perturbation of the plasma-membrane-proximal F-actin network, a process that has previously been described to directly regulate BCR signaling (Fig. 4*L* and *SI Appendix*, Fig. S4*E*).

Discussion

RHOA is involved in various cellular pathways including the regulation of the actin cytoskeleton dynamics, receptor endocytosis, and cell migration (12). This study was motivated by our findings, i) that lymphoma cells are more dependent on RHOA function than other cancer types, and ii) that DLBCL tumors show recurrent mutations in *RHOA* and its activators, both suggesting an important role of RHOA in DLBCL biology.

By combining functional genomics, proteomics, and superresolution microscopy, we have elucidated the functional role of RHOA and its mutant variants in DLBCL. We identified RHOA as a master regulator of oncogenic chronic active BCR signaling in ABC DLBCL. Interestingly, RHOA controls two central mechanisms: First, the spatial organization of the plasma membrane-bound BCR within active microclusters that were previously shown to be essential for proximal BCR signaling (3, 4). Second, BCR endocytosis as a requirement for the function of the My-T-BCR complex that forms intracellularly, consisting of the internalized BCR, TLR9, and MYD88, and is essential for oncogenic NF-κB signaling in a subset of ABC DLBCLs. Previous studies have demonstrated that BCR endocytosis can be mediated by either clathrin-dependent or

independent pathways (80–82). While constitutive BCR endocytosis is largely controlled by clathrin-dependent mechanisms (83), activated BCRs are mostly internalized in a clathrin-independent manner because the phosphorylation of the ITAMs within CD79A/B counteracts the binding of AP2, which is the key adaptor protein responsible for the initiation of clathrin-dependent endocytosis. Given the chronic activation of BCRs in ABC DLBCL cells, it is likely that clathrin-independent pathways significantly contribute to BCR endocytosis in these cells. This endocytosis mode is known to be particularly dependent on actin reorganization, and previous studies have demonstrated that clathrin-independent endocytosis of receptors other than the BCR is regulated by RHOA (84, 85). Hence, our data suggest that RHOA is essential for My-T-BCR function, because it controls BCR endocytosis, most likely in a clathrin-independent manner, to allow internalized BCRs to assemble within the My-T-BCR complex. However, the detailed mechanisms how RHOA regulates BCR clustering and internalization beyond the regulation of the actin cytoskeleton remain unclear and should be explored in future studies.

The functional relevance of RHOA is further underscored by the occurrence of *RHOA* mutations in DLBCL. The *RHOA* R5W mutation, which is found in ABC DLBCL, affects an arginine in the first beta-sheet, which is important for GEF binding and thus RHOA activation (86). Accordingly, we found that this particular mutation enhanced BCR microcluster formation, thereby strengthening the oncogenic BCR signaling output. Enhanced BCR clustering in DLBCL cells expressing the RHOA R5W mutant is caused by a reorganization of the cortical actin network, shifting the balance from F-actin toward G-actin. F-actin is known to restrict the lateral movement of cell surface BCRs thereby inhibiting the formation and the signaling output of BCR microclusters (26, 87), which has secondary effects on BCR endocytosis (26, 87). Shifting the balance from F- to G-actin thus unleashes an amplified BCR signal due to the breakup of inhibitory plasma membrane compartments that are mediated by the cortical F-actin fence. It remains unclear whether mutant RHOA does additionally influence the BCR-proximal membrane lipid composition through rewiring of the actin network which could be another important mechanism affecting the BCR signaling output.

An important question in the context of precision medicine is whether *RHOA* mutations would affect the response to compounds targeting oncogenic BCR signaling, such as BTK inhibitors. These have proven efficacy in clinical trials, especially in ABC DLBCL harboring mutations in *MYD88* and *CD79B* (15). *RHOA* mutations may identify tumors with enhanced BCR signaling that in theory could be more sensitive to BTK inhibition due to a stronger BCR dependency. However, our data suggest that the R5W hotspot mutation renders DLBCL cells less responsive to BTK inhibitors in vitro, pointing toward a less sufficient suppression of BCR signaling by BTK inhibitors once the pathway is hyperactivated by mutant (R5W) RHOA.

A limitation of this study is that the mechanistic insights presented are based on lymphoma cell line models. While these models capture important genetic and signaling features of ABC DLBCL, they do not fully reflect the complexity of primary tumors, including the intratumoral heterogeneity and microenvironmental factors.

Interestingly, a plethora of different *RHOA* mutations is found in ABC and GCB DLBCL (Fig. 4*A* and *SI Appendix*, Fig. S4*A*), and they likely act through different mechanisms given the distinct biology of these DLBCL subtypes. This is supported by our data revealing functional differences between the R5W and L69P variants. Our functional and biochemical analyses revealed a gain-of-function phenotype for the p.R5W RHOA mutant in ABC DLBCL, resulting in enhanced BCR clustering at the cell surface and an increased My-T-BCR signaling output. Interestingly, the same mutation also occurs in GCB DLBCL, a subtype known to lack the expression of the My-T-BCR complex, but still being dependent on cell surface BCR signaling. While we have not explored the functional impact of *RHOA* mutations in GCB DLBCL, it is tempting to speculate that mutant RHOA influences BCR-driven survival signals in GCB DLBCL as well, potentially through alternative mechanisms though. *RHOA* mutations are also found in T cell lymphoma, most frequently in angioimmunoblastic T-NHL (AITL). However, the mutational spectrum markedly differs between B and T cell lymphoma. While DLBCL hotspot mutations often affect the amino acid residues R5 and L69, AITL is almost exclusively associated with G17V alteration. This particular AITL-associated mutation leads to enhanced PI3-kinase signaling through activation of ICOS and VAV1 (88). The marked differences between the mutation types found in DLBCL and AITL suggest distinct pathomechanistic features, and future studies are needed to functionally annotate the manifold *RHOA* mutations occurring in lymphoma. The different mutations in B and T cell lymphomas, however, suggest the possibility that they interact with different GEFs, GDIs, or other proteins. Therefore, there may be opportunities to interfere specifically with mutant RHOA function in malignant B and T cells without affecting WT RHOA function in other cell types.

Methods

Additional details are available in the *SI Appendix, Materials and Methods*.

Cell Culture. All lymphoma cell lines were provided by Louis Staudt (NIH, Bethesda). All cells were grown in advanced RPMI medium with either 5% or 10% fetal bovine serum (FBS) + 1% penicillin/streptomycin and 2 mM L-Glutamine. HEK293FT (Takara/Clontech) and HEK293T cells (ThermoFisher) were cultured in Dulbecco's modified Eagle medium (DMEM) with 10% FBS (Merck) and 2 mM L-Glutamine.

Virus Production. Lentivirus was made by using HEK293FT cells, transfecting with pMD2.G (Addgene plasmid #1225) and psPAX2 (Addgene plasmid # 12260) gag/pol and envelope plasmids using OptiMEM medium (Life Technologies) and TransIT293 (Mirus) transfection reagent following the manufacturer's instructions. Lentiviral particles were harvested on all three following days and concentrated using Lenti-X concentrator (TaKaRa) or ultracentrifuged (30,000 rpm, 2 h 15 min, 4 °C). Retrovirus was made by using HEK293T cells that were transfected with TransIT293 transfection reagent with pHIT-60/full-length GALV or pHIT-60/EA6x3* helper plasmids. Retroviral supernatant was harvested after (shRNA) 24–48 h or (BioID2) every 24 h for 3 d. To infect lymphoma cell lines with shRNA containing virus, cells were spin-infected by centrifugation (90 min, 2,500 rpm). For BioID2 constructs, viral supernatant was spun on retronectin (TaKaRa)-coated nontissue-treated plates (3×, 2,500 rpm, 32 °C, 30 min) and then, cells transduced via centrifugation on the retronectin plate (1,000 rpm, 5 min).

Generation of Mutant Knock-In Cell Lines. An sgRNA was designed in Benchling targeting the region around the desired mutation and ordered from IDT along with Cas9 protein, an HDR template (100 to 110 bp Ultramers with phosphorothioate modifications), and electroporation enhancers. RNP complexes were assembled by incubating Cas9 with sgRNA and combined with HDR templates and enhancer prior to electroporation. Approximately 5×10^5 cells were resuspended in Buffer R and electroporated using a Neon Transfection System with optimized settings for each cell line. Following electroporation, cells were cultured in complete media supplemented with HDR enhancer and conditioned medium until they recovered. Pools were optionally PCR-screened for editing

efficiency before plating at limiting dilution for single-cell expansion. Individual clones were lysed, and target regions were PCR-amplified and analyzed by Sanger sequencing to identify positive knock-in clones.

Data, Materials, and Software Availability. RNA-sequencing data have been deposited in GEO (accession number: GSE306747) (89). Proteomics data have been deposited in MassIVE (accession number: MSV000100447) (90). Other data are included in the article and/or supporting information.

ACKNOWLEDGMENTS. This study was funded by the Hessian research support program *LOEWE* (funding reference number LOEWE/2/17/519/03/10.001(0004)/111) and by the Deutsche Forschungsgemeinschaft (DFG, German Research Foundation) SFB1530, Project A02, funding references 455784452 and 548257578. This work was supported by a Grant from the Else Kröner-Fresenius-Stiftung (2024_EKEA.43).

Author affiliations: [a]Department of Medicine 2, Hematology/Oncology, University Medical Center Frankfurt, Goethe University, Frankfurt am Main 60590, Germany; [b]Frankfurt Cancer Institute, Goethe University Frankfurt, Frankfurt am Main 60590, Germany; [c]German Cancer Consortium, Partner Site Frankfurt/Mainz and German Cancer Research Center, Heidelberg 60590, Germany; [d]Institute for Cellular and Molecular Immunology, University Medical Center Göttingen, Göttingen 37075, Germany; [e]Lymphoid Malignancies Branch, National Cancer Institute, National Institutes of Health, Bethesda, MD 20892; [f]Department of Hematology, Oncology and Tumor Immunology, Charité University Medical Center, Berlin 12203, Germany; and [g]University Cancer Center Frankfurt, University Medical Center Frankfurt, Goethe University, Frankfurt am Main 60590, Germany

Author contributions: S.S. and T.O. designed research; A.N.J., D.J., T.B., R.K.K., M.E., B.H., S.M., N.D., M.P., M.B., X.Y., N.S., R.W.-K., A.Z., C.D., B.C., and S.S. performed research; A.N.J., D.J., T.B., S.W., L.M.S., S.S., and T.O. analyzed data; and A.N.J., L.M.S., S.S., and T.O. wrote the paper.

Reviewers: M.R.G., The University of Texas MD Anderson Cancer Center Endocrine Center; and S.P., Massachusetts General Hospital.

1. G. Lenz, L. M. Staudt, Aggressive lymphomas. *N. Engl. J. Med.* **362**, 1417–1429 (2010), 10.1056/NEJMra0807082.
2. A. A. Alizadeh *et al.*, Distinct types of diffuse large B-cell lymphoma identified by gene expression profiling. *Nature* **403**, 503–511 (2000), 10.1038/35000501.
3. S. Scheich *et al.*, Targeting N-linked glycosylation for the therapy of aggressive lymphomas. *Cancer Discov.* **13**, 1862–1883 (2023), 10.1158/2159-8290.CD-22-1401.
4. R. E. Davis *et al.*, Chronic active B-cell-receptor signalling in diffuse large B-cell lymphoma. *Nature* **463**, 88–92 (2010), 10.1038/nature08638.
5. R. M. Young *et al.*, Taming the heterogeneity of aggressive lymphomas for precision therapy. *Annu. Rev. Cancer Biol.* **3**, 429–455 (2019), 10.1146/annurev-cancerbio-030518-055734.
6. N. D. Perkins, Integrating cell-signalling pathways with NF-kappaB and IKK function. *Nat. Rev. Mol. Cell Biol.* **8**, 49–62 (2007), 10.1038/nrm2083.
7. B. Chapuy *et al.*, Molecular subtypes of diffuse large B cell lymphoma are associated with distinct pathogenic mechanisms and outcomes. *Nat. Med.* **24**, 679–690 (2018), 10.1038/s41591-018-0016-8.
8. R. Schmitz *et al.*, Genetics and pathogenesis of diffuse large B-cell lymphoma. *N. Engl. J. Med.* **378**, 1396–1407 (2018), 10.1056/NEJMoa1801445.
9. G. W. Wright *et al.*, A probabilistic classification tool for genetic subtypes of diffuse large B cell lymphoma with therapeutic implications. *Cancer Cell* **37**, 551–568.e514 (2020), 10.1016/j.ccell.2020.03.015.
10. B. Chapuy *et al.*, DLBclass: A probabilistic molecular classifier to guide clinical investigation and practice in diffuse large B-cell lymphoma. *Blood* **145**, 2041–2055 (2025), 10.1182/blood.2024025652.
11. J. D. Phelan *et al.*, A multiprotein supercomplex controlling oncogenic signalling in lymphoma. *Nature* **560**, 387–391 (2018), 10.1038/s41586-018-0290-0.
12. J. Wei *et al.*, A new mechanism of RhoA ubiquitination and degradation: Roles of SCF(FBXL19) E3 ligase and Erk2. *Biochim. Biophys. Acta* **1833**, 2757–2764 (2013), 10.1016/j.bbamcr.2013.07.005.
13. M. Nakagawa *et al.*, Targeting the HTLV-I-regulated BATF3/IRF4 transcriptional network in adult T cell leukemia/lymphoma. *Cancer Cell* **34**, 286–297.e210 (2018), 10.1016/j.ccell.2018.06.014.
14. Y. Yang *et al.*, Oncogenic RAS commandeers amino acid sensing machinery to aberrantly activate mTORC1 in multiple myeloma. *Nat. Commun.* **13**, 5469 (2022), 10.1038/s41467-022-33142-x.
15. W. H. Wilson *et al.*, Effect of ibrutinib with R-CHOP chemotherapy in genetic subtypes of DLBCL. *Cancer Cell* **39**, 1643–1653.e1643 (2021), 10.1016/j.ccell.2021.10.006.
16. DepMap consortium–Cancer Dependency Map Portal (2023), https://depmap.org/portal/.
17. X. Shang *et al.*, Small-molecule inhibitors targeting G-protein-coupled rho guanine nucleotide exchange factors. *Proc. Natl. Acad. Sci. U.S.A.* **110**, 3155–3160 (2013), 10.1073/pnas.1212324110.
18. T. C. Francis, A. Gaynor, R. Chandra, M. E. Fox, M. K. Lobo, The selective RhoA inhibitor rhosin promotes stress resiliency through enhancing D1-medium spiny neuron plasticity and reducing hyperexcitability. *Biol. Psychiatry* **85**, 1001–1010 (2019), 10.1016/j.biopsych.2019.02.007.
19. Y. Baba *et al.*, BLNK mediates Syk-dependent Btk activation. *Proc. Natl. Acad. Sci. U.S.A.* **98**, 2582–2586 (2001), 10.1073/pnas.051626198.
20. C. Fu, C. W. Turck, T. Kurosaki, A. C. Chan, BLNK: A central linker protein in B cell activation. *Immunity* **9**, 93–103 (1998), 10.1016/s1074-7613(00)80591-9.
21. M. Maekawa *et al.*, Signaling from rho to the actin cytoskeleton through protein kinases ROCK and LIM-kinase. *Science* **285**, 895–898 (1999), 10.1126/science.285.5429.895.
22. J. Seze, J. Gatin, M. Coppey, RhoA regulation in space and time. *FEBS Lett.* **597**, 836–849 (2023), 10.1002/1873-3468.14578.
23. G. Lenz *et al.*, Oncogenic CARD11 mutations in human diffuse large B cell lymphoma. *Science* **319**, 1676–1679 (2008), 10.1126/science.1153629.
24. K. Rinaldi, A. Bolomsky, J. Wisniewski, L. Zhang, R. M. Young, Use of proximity ligation assay to study lymphoid malignancies. *Methods Mol. Biol.* **2865**, 273–282 (2025), 10.1007/978-1-0716-4188-0_12.
25. P. K. Mattila *et al.*, The actin and tetraspanin networks organize receptor nanoclusters to regulate B cell receptor-mediated signaling. *Immunity* **38**, 461–474 (2013), 10.1016/j.immuni.2012.11.019.
26. B. Treanor *et al.*, The membrane skeleton controls diffusion dynamics and signaling through the B cell receptor. *Immunity* **32**, 187–199 (2010), 10.1016/j.immuni.2009.12.005.
27. M. Sakata-Yanagimoto *et al.*, Somatic RHOA mutation in angioimmunoblastic T cell lymphoma. *Nat. Genet.* **46**, 171–175 (2014), 10.1038/ng.2872.
28. T. Palomero *et al.*, Recurrent mutations in epigenetic regulators, RHOA and FYN kinase in peripheral T cell lymphomas. *Nat. Genet.* **46**, 166–170 (2014), 10.1038/ng.2873.
29. R. Dvorsky, M. R. Ahmadian, Always look on the bright site of Rho: Structural implications for a conserved intermolecular interface. *EMBO Rep.* **5**, 1130–1136 (2004), 10.1038/sj.embor.7400293.
30. S. E. Arthur *et al.*, Genome-wide discovery of somatic regulatory variants in diffuse large B-cell lymphoma. *Nat. Commun.* **9**, 4001 (2018), 10.1038/s41467-018-06354-3.
31. B. Collinge *et al.*, High-grade B-cell lymphoma, not otherwise specified: An LLMPP study. *Blood Adv.* **9**, 5409–5422 (2025), 10.1182/bloodadvances.2025016651.
32. A. Cooper *et al.*, CD5 gene signature identifies diffuse large B-cell lymphomas sensitive to BrutonÊ¼s tyrosine kinase inhibition. *J. Clin. Oncol.* **42**, 467–480 (2024), 10.1200/JCO.23.01574.
33. F. Cucco *et al.*, Distinct genetic changes reveal evolutionary history and heterogeneous molecular grade of DLBCL with MYC/BCL2 double-hit. *Leukemia* **34**, 1329–1341 (2020), 10.1038/s41375-019-0691-6.
34. A. R. Davis *et al.*, Targeted massively parallel sequencing of mature lymphoid neoplasms: Assessment of empirical application and diagnostic utility in routine clinical practice. *Mod. Pathol.* **34**, 904–921 (2021), 10.1038/s41379-020-00720-7.
35. K. Dreval *et al.*, Genetic subdivisions of follicular lymphoma defined by distinct coding and noncoding mutation patterns. *Blood* **142**, 561–573 (2023), 10.1182/blood.2022018719.
36. D. Ennishi *et al.*, Double-hit gene expression signature defines a distinct subgroup of germinal center B-cell-like diffuse large B-cell lymphoma. *J. Clin. Oncol.* **37**, 190–201 (2019), 10.1200/JCO.18.01583.
37. F. Gao, K. Hu, P. Zheng, H. Shi, X. Ke, Characteristics and prognosis of rrDLBCL with TP53 mutations and a high-risk subgroup represented by the co-mutations of DDX3X-TP53. *Cancer Med.* **12**, 10267–10279 (2023), 10.1002/cam4.5756.
38. J. González-Rincón *et al.*, Unraveling transformation of follicular lymphoma to diffuse large B-cell lymphoma. *PLoS One* **14**, e0212813 (2019), 10.1371/journal.pone.0212813.
39. D. M. Greenawalt *et al.*, Comparative analysis of primary versus relapse/refractory DLBCL identifies shifts in mutation spectrum. *Oncotarget* **8**, 99237–99244 (2017), https://doi.org/10.18632/oncotarget.18502.
40. E. Güney *et al.*, A genetically distinct pediatric subtype of primary CNS large B-cell lymphoma is associated with favorable clinical outcome. *Blood Adv.* **6**, 3189–3193 (2022), 10.1182/bloodadvances.2021006018.
41. L. K. Hilton *et al.*, Relapse timing is associated with distinct evolutionary dynamics in DLBCL. medRxiv [Preprint] (2023) https://doi.org/10.1101/2023.03.06.23286584 (Accessed 30 November 2025).
42. A. M. Intlekofer *et al.*, Integrated DNA/RNA targeted genomic profiling of diffuse large B-cell lymphoma using a clinical assay. *Blood Cancer J.* **8**, 60 (2018), 10.1038/s41408-018-0089-0.
43. S. Jiang *et al.*, Molecular profiling of Chinese R-CHOP treated DLBCL patients: Identifying a high-risk subgroup. *Int. J. Cancer* **147**, 2611–2620 (2020), 10.1002/ijc.33049.
44. D. Juskevicius *et al.*, Distinct genetic evolution patterns of relapsing diffuse large B-cell lymphoma revealed by genome-wide copy number aberration and targeted sequencing analysis. *Leukemia* **30**, 2385–2395 (2016), 10.1038/leu.2016.135.
45. D. Juskevicius *et al.*, Mutations of CREBBP and SOCS1 are independent prognostic factors in diffuse large B cell lymphoma: Mutational analysis of the SAKK 38/07 prospective clinical trial cohort. *J. Hematol. Oncol.* **10**, 70 (2017), 10.1186/s13045-017-0438-7.
46. K. Kataoka *et al.*, Frequent structural variations involving programmed death ligands in Epstein-Barr virus-associated lymphomas. *Leukemia* **33**, 1687–1699 (2019), 10.1038/s41375-019-0380-5.
47. A. Künstner *et al.*, Mutational landscape of high-grade B-cell lymphoma with MYC-, BCL2 and/or BCL6 rearrangements characterized by whole-exome sequencing. *Haematologica* **107**, 1850–1863 (2021), 10.3324/haematol.2021.279631.
48. S. E. Lacy *et al.*, Targeted sequencing in DLBCL, molecular subtypes, and outcomes: A Haematological Malignancy Research Network report. *Blood* **135**, 1759–1771 (2020), 10.1182/blood.2019003535.
49. D. J. Landsburg *et al.*, Mutation analysis performed on tumor biopsies from patients with newly-diagnosed germinal center aggressive B cell lymphomas. *Oncotarget* **13**, 1237–1244 (2022), https://doi.org/10.18632/oncotarget.28309.
50. M. S. Lionakis *et al.*, Inhibition of B cell receptor signaling by ibrutinib in primary central nervous system lymphoma. *Cancer Cell* **31**, 833–843.e5 (2017), 10.1016/j.ccell.2017.04.012.
51. G. T. Los-de Vries *et al.*, Large b-cell lymphomas of immune-privileged sites relapse via parallel clonal evolution from a common progenitor b cell. *Cancer Res.* **83**, 1917–1927 (2023), 10.1158/0008-5472.CAN-22-3814.
52. M. C. J. Ma *et al.*, Subtype-specific and co-occurring genetic alterations in B-cell non-Hodgkin lymphoma. *Haematologica* **107**, 690–701 (2021), 10.3324/haematol.2020.274258.
53. C. Melani *et al.*, Combination targeted therapy in relapsed diffuse large B-cell lymphoma. *N. Engl. J. Med.* **390**, 2143–2155 (2024), 10.1056/NEJMoa2401532.
54. M. Mendeville *et al.*, The path towards consensus genome classification of diffuse large B-cell lymphoma for use in clinical practice. *Front. Oncol.* **12**, 970063 (2022), 10.3389/fonc.2022.970063.
55. T. Menter *et al.*, Mutational landscape of B-cell post-transplant lymphoproliferative disorders. *Br. J. Haematol.* **178**, 48–56 (2017), 10.1111/bjh.14633.
56. R. D. Morin *et al.*, Mutational and structural analysis of diffuse large B-cell lymphoma using whole-genome sequencing. *Blood* **122**, 1256–1265 (2013), 10.1182/blood-2013-02-483727.
57. T. Nakamura *et al.*, Recurrent mutations of CD79B and MYD88 are the hallmark of primary central nervous system lymphomas. *Neuropathol. Appl. Neurobiol.* **42**, 279–290 (2016), 10.1111/nan.12259.

58. J. Okosun *et al.*, Integrated genomic analysis identifies recurrent mutations and evolution patterns driving the initiation and progression of follicular lymphoma. *Nat. Genet.* **46**, 176–181 (2014), 10.1038/ng.2856.
59. E. M. Parry *et al.*, Evolutionary history of transformation from chronic lymphocytic leukemia to Richter syndrome. *Nat. Med.* **29**, 158–169 (2023), 10.1038/s41591-022-02113-6.
60. A. A. Pomares *et al.*, Genetic subtyping by whole exome sequencing across diffuse large B cell lymphoma and plasmablastic lymphoma. *PLoS One* **20**, e0318689 (2025), 10.1371/journal.pone.0318689.
61. A. Reddy *et al.*, Genetic and functional drivers of diffuse large B cell lymphoma. *Cell* **171**, 481–494. e15 (2017). 10.1016/j.cell.2017.09.027.
62. A. Rivas-Delgado *et al.*, Mutational landscape and tumor burden assessed by cell-free DNA in diffuse large B-cell lymphoma in a population-based study. *Clin. Cancer Res.* **27**, 513–521 (2021), 10.1158/1078-0432.CCR-20-2558.
63. A. Rivas-Delgado *et al.*, Testicular large B-cell lymphoma is genetically similar to PCNSL and distinct from nodal DLBCL. *Hemasphere* **8**, e70024 (2024), 10.1002/hem3.70024.
64. C. K. Rushton *et al.*, Genetic and evolutionary patterns of treatment resistance in relapsed B-cell lymphoma. *Blood Adv.* **4**, 2886–2898 (2020), 10.1182/bloodadvances.2020001696.
65. R. Sciarra *et al.*, Molecular characterization of diffuse large B-cell lymphomas associated with hepatitis C virus infection. *Br. J. Haematol.* **204**, 2242–2253 (2024), 10.1111/bjh.19378.
66. C. Sha *et al.*, Molecular high-grade B-cell lymphoma: Defining a poor-risk group that requires different approaches to therapy. *J. Clin. Oncol.* **37**, 202–212 (2019), 10.1200/JCO.18.01314.
67. H. Shi *et al.*, Genetic landscapes and curative effect of CAR T-cell immunotherapy in patients with relapsed or refractory DLBCL. *Blood Adv* **7**, 1070–1075 (2022), 10.1182/bloodadvances.2021006845.
68. The AACR Project GENIE Consortium *et al.*, AACR Project GENIE: Powering precision medicine through an international consortium. *Cancer Discov.* **7**, 818–831 (2017), 10.1158/2159-8290.CD-17-0151.
69. X. Ye *et al.*, Genome-wide mutational signatures revealed distinct developmental paths for human B cell lymphomas. *J. Exp. Med.* **218**, e20200573 (2020). 10.1084/jem.20200573.
70. J. Zhang *et al.*, Genetic heterogeneity of diffuse large B-cell lymphoma. *Proc. Natl. Acad. Sci. U.S.A.* **110**, 1398–1403 (2013), 10.1073/pnas.1205299110.
71. X. A. Zhou *et al.*, Genomic analyses identify recurrent alterations in immune evasion genes in diffuse large B cell lymphoma. Leg type. *J. Invest. Dermatol.* **138**, 2365–2376 (2018), 10.1016/j.jid.2018.04.038.
72. Y. Zhou *et al.*, Analysis of genomic alteration in primary central nervous system lymphoma and the expression of some related genes. *Neoplasia* **20**, 1059–1069 (2018), 10.1016/j.neo.2018.08.012.
73. A. Künstner *et al.*, Molecular profiling of primary renal diffuse large B-cell lymphoma unravels a proclivity for immune-privileged tropism. *Blood Adv* **9**, 3900–3904 (2025), 10.1182/bloodadvances.2025016002.
74. W. Lone *et al.*, High-grade B-cell lymphoma not otherwise specified, with diffuse large B-cell lymphoma gene expression signatures: Genomic analysis and potential therapeutics. *Am. J. Hematol.* **100**, 10–22 (2025), 10.1002/ajh.27513.
75. X. D. Ren, W. B. Kiosses, M. A. Schwartz, Regulation of the small GTP-binding protein Rho by cell adhesion and the cytoskeleton. *EMBO J.* **18**, 578–585 (1999), 10.1093/emboj/18.3.578.
76. A. L. Shaffer *et al.*, A library of gene expression signatures to illuminate normal and pathological lymphoid biology. *Immunol. Rev.* **210**, 67–85 (2006), 10.1111/j.0105-2896.2006.00373.x.
77. H. Lu, H. Huang, FOXO1: A potential target for human diseases. *Curr. Drug Targets* **12**, 1235–1244 (2011), 10.2174/138945011796150280.
78. J. Zhang *et al.*, Characterizing the topography of membrane receptors and signaling molecules from spatial patterns obtained using nanometer-scale electron-dense probes and electron microscopy. *Micron* **37**, 14–34 (2006), 10.1016/j.micron.2005.03.014.
79. M. A. Kiskowski, J. F. Hancock, A. K. Kenworthy, On the use of Ripley's K-function and its derivatives to analyze domain size. *Biophys. J.* **97**, 1095–1103 (2009), 10.1016/j.bpj.2009.05.039.
80. D. Malinova *et al.*, Endophilin A2 regulates B-cell endocytosis and is required for germinal center and humoral responses. *EMBO Rep.* **22**, e51328 (2021), 10.15252/embr.202051328.
81. A. D. Roberts *et al.*, Structurally distinct endocytic pathways for B cell receptors in B lymphocytes. *Mol. Biol. Cell.* **31**, 2826–2840 (2020), 10.1091/mbc.E20-08-0532.
82. A. Stoddart, A. P. Jackson, F. M. Brodsky, Plasticity of B cell receptor internalization upon conditional depletion of clathrin. *Mol. Biol. Cell* **16**, 2339–2348 (2005), 10.1091/mbc.e05-01-0025.
83. A. D. Roberts, J. W. Taraska, B cell receptor (BCR) endocytosis. *Prog. Mol. Biol. Transl. Sci.* **194**, 159–177 (2023), 10.1016/bs.pmbts.2022.08.003.
84. D. C. Prosser, B. Wendland, Conserved roles for yeast Rho1 and mammalian RhoA GTPases in clathrin-independent endocytosis. *Small GTPases* **3**, 229–235 (2012), 10.4161/sgtp.21631.
85. S. Mayor, R. G. Parton, J. G. Donaldson, Clathrin-independent pathways of endocytosis. *Cold Spring Harb. Perspect. Biol.* **6**, a016758 (2014), 10.1101/cshperspect.a016758.
86. M. O'Hayre *et al.*, Inactivating mutations in GNA13 and RHOA in Burkitt's lymphoma and diffuse large B-cell lymphoma: a tumor suppressor function for the Galpha13/RhoA axis in B cells. *Oncogene* **35**, 3771–3780 (2016).
87. W. Song *et al.*, Actin-mediated feedback loops in B-cell receptor signaling. *Immunol. Rev.* **256**, 177–189 (2013), 10.1111/imr.12113.
88. M. Fujisawa *et al.*, Activation of RHOA-VAV1 signaling in angioimmunoblastic T-cell lymphoma. *Leukemia* **32**, 694–702 (2018), 10.1038/leu.2017.273.
89. A. Jacobs *et al.*, RHOA controls oncogenic B cell receptor signaling in aggressive lymphoma. Gene Expression Omnibus. https://www.ncbi.nlm.nih.gov/geo/query/acc.cgi?acc=GSE306747. Deposited 28 August 2025.
90. A. Jacobs *et al.*, RHOA controls oncogenic B cell receptor signaling in aggressive lymphoma. MassIVE. https://massive.ucsd.edu. Deposited 13 January 2026.